Critical Behavior at a Valence Instability*

J. M. Lawrence, M. C. Croft, and R. D. Parks
Department of Physics and Astronomy, University of Rochester, Rochester, New York 14627
(Received 19 May 1975)

The isomorphic phase transition in the system $Ce_{1-x}Th_x$, which is characterized by a delocalization of the $4f$ electron and a concomitant volume change, has been studied through measurements of the density and resitivity. For samples near the critical composition ($x \simeq 0.264$) derivatives of these quantities diverge with mean-field exponents. Such mean-field behavior implies a long-force range, and suggests that electroelastic coupling dominates the critical behavior.

Considerable attention has been given recently[1-4] to the samarium chalcogenides and related structures which exhibit isomorphic phase transitions characterized by the delocalization of a $4f$ electron. A large fraction of this effort has been concerned with the elucidation of the properties of the collapsed phase, which appears to be characterized by the configurational mixing of ionic $4f$ states with itinerant $6s$ or $5d$ states.[5,6] The focus in the present work is the phase transition itself, not in the Sm chalcogenides but in the system $Ce_{1-x}Th_x$ which exhibits similar behavior. We have been able to (1) identify the critical concentration ($x_c = 0.264$), i.e., the concentration for which the transition is second order, and (2) measure various thermodynamic divergences near the critical point T_c over two decades in reduced temperature $\epsilon = |T - T_c|/T_c$.

It has long been known that cerium itself undergoes an isomorphic (fcc→fcc) transition[7] similar to that observed more recently in the Sm chalcogenides. The transition is first order under ambient conditions but can be made second order by the application of pressure or by alloying with thorium.[8,9] In the x-T plane the phase boundary of $Ce_{1-x}Th_x$ which separates the "collapsed" (α) state from the higher-temperature (γ) state (the latter being characterized by a greater degree of localization of the $4f$ electron) appears as a line of first-order transitions which terminates in a critical point. When the transition is first order it is characterized, as in the Sm chalcogenides or in pure cerium itself, by relatively large changes in the volume (~15%), magnetic susceptibility, and transport coefficients such as resistivity.

Samples were prepared by arc melting followed by vacuum anneals at 600°C for two weeks. Thorium in concentrations greater than 10% is known to eliminate the double-hcp β phase[8] which complicates analyses in pure cerium; and, indeed, room-temperature x-ray examination of samples cycled through the transition revealed only one fcc phase present.

That portion of the x-T phase diagram which includes the region of interest was determined from resistivity measurements. In Fig. 1 we show data for four alloys with thorium concentrations bracketing x_c. As $x \to x_c$ from below the well-defined first-order step shrinks to zero and as $x \to x_c$ from above, the peak in the tempearture derivative [Fig. 2(a)] of the S-shaped $R(T)$ curve approaches a true divergence. Thus, given that $R(T)$ is coupled linearly to the order parameter $\rho(T)$ (the density)—and we shall demonstrate this linear coupling below—we see that the isoconcentration curves $R(T)$ are entirely analogous to the isobaric curves $V(T)$ for the liquid-gas transition. In Fig. 2(b) we extrapolate $1/(dR/dT)_{max}$ to zero

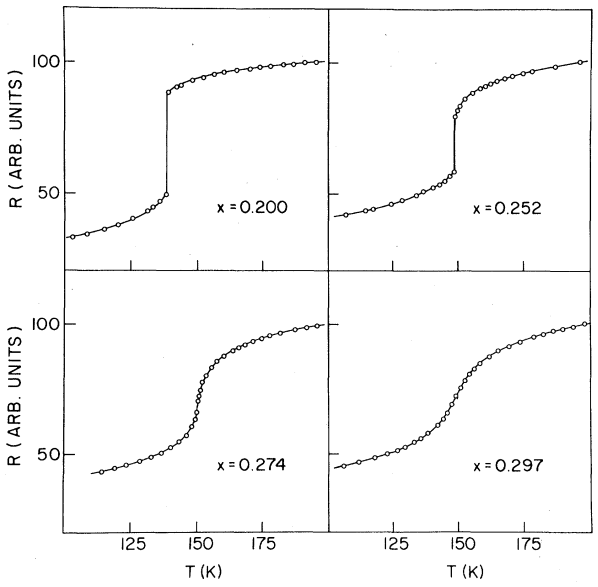

FIG. 1. Resistivity versus temperature for samples near the critical composition in the $Ce_{1-x}Th_x$ system.

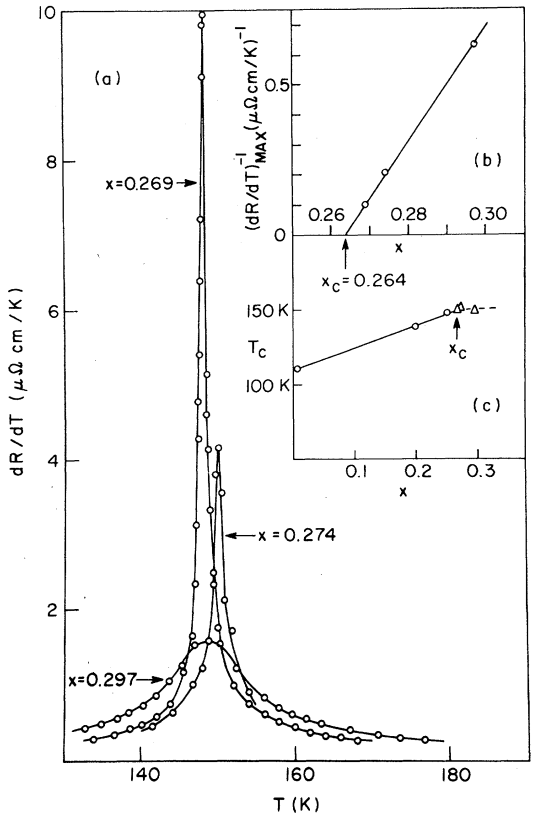

FIG. 2. (a) dR/dT for samples with $x \gtrsim x_c$; (b) $(dR/dT)_{max}^{-1}$ versus x and extrapolated to zero to give estimate of x_c; (c) phase boundary where circles correspond to first-order transitions and triangles to continous transitions.

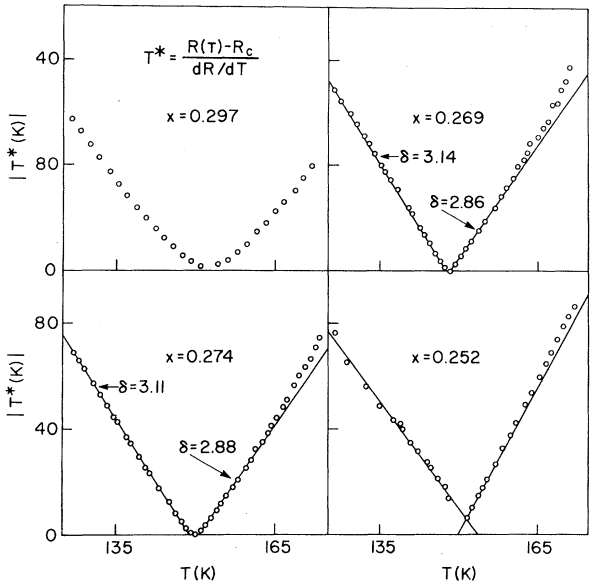

FIG. 3. $|T^*(T)|$ versus T in the vicinity of T_c for four samples. The slopes of the straight lines give the exponent δ.

and arrive at an estimate of the critical concentration, $x = 0.264 \pm 0.003$. We then have the phase diagram of Fig. 2(c), where we have plotted the line of first-order transitions which terminates at the critical concentration. We have extended this line into "continous transition space" by plotting the points (x,T) corresponding to the observed maxima in dR/dT.

Pursuing the analogy to liquid-vapor isobars, we expect the isoconcentration curves in the critical region to have the form[10]

$$A(\Delta R)^{\delta} + B\,\Delta x\,\Delta R \propto T - T_c, \qquad (1)$$

where for volume we have substituted resistivity R and for pressure, concentration x, and where $\Delta R = R - R_c$ and $\Delta x = x - x_c$, R_c and x_c being the critical values. For $\Delta x = 0$ we would have a true divergence, giving us the well-known δ exponent. The term linear in ΔR removes the divergence for $x \neq x_c$; it is essentially a Van der Waals rounding term.[10] *A posteriori* we can justify applying a Van der Waals analysis because of the observed mean-field behavior as discussed below. We have chosen to analyze our data in terms of the function of $T^*(T) = \Delta R/(dR/dT)$. For a system obeying Eq. (1), we have $T^*(T) = \delta(T - T_c) + (1 - \delta)B\Delta x \Delta R$. Far enough from T_c this should give a straight line with slope δ but intercepts $T_{c\pm} = T_c \pm [(\delta - 1)/\delta]B\Delta x\,\Delta R$; in close to T_c it will exhibit rounding. As $\Delta x \to 0$ rounding decreases and the intercepts move in until for $x = x_c$ we should have two straight lines, above and below T_c, both with slope δ and both extrapolating to zero at T_c. For negative Δx (first-order transitions) the intercepts move to the other side of T_c; i.e., the lines cross.

As is seen in Fig. 3 and 4 the data exhibit all these features: As $x \to x_c$ the rounding decreases dramatically, the values of $T_{c\pm}$ approach T_c, and the $x = 0.252$ sample shows the mentioned crossover. The $x = 0.274$ sample is already sufficiently close to x_c that we see a well-defined exponent δ fitting over a decade below T_c ($2 \times 10^{-2} < \epsilon < 2 \times 10^{-1}$). [The upturn in $T^*(T)$ is present in all samples studied; it is a background effect peculiar to resistivity.] At $x = 0.269$ the fit is now good over two decades but the exponent remains unchanged. Therefore, by this method, we have found the exponent δ even though we have not examined the data for the critical concentration it-

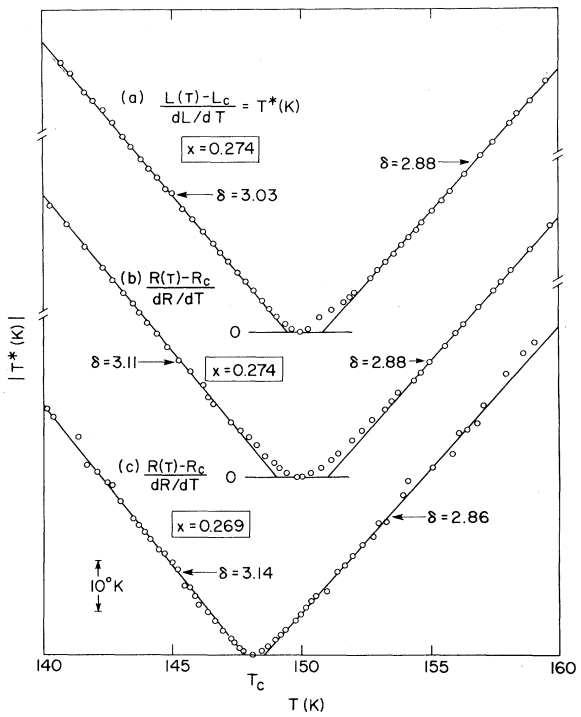

FIG. 4. $|T^*(T)|$ for (a) length measurement, $x = 0.274$; (b) resistivity, $x = 0.274$; and (c) resistivity, $x = 0.269$.

self. This is analogous to determining δ for a ferromagnet from $M(H)$ curves taken close to but not precisely at T_c and extracting δ from the equation of state. Taking account of asymmetry by taking the mean of the values of δ above and below T_c, we have $\delta = 3.0 \pm 0.2$ for $4\times10^{-3} < \epsilon < 2\times10^{-1}$. This is the value for mean-field behavior ($\delta = 3$) as compared to $\delta \simeq 4.2$ for liquid-gas transitions and $\delta \simeq 5$ for Ising-model calculations.

Shown also in Fig. 4 is a plot of T^* for the length measurement $L(T)$ on the sample with $x = 0.274$; the data were obtained by the method of capacitive dilatometry. This is an important measurement since the density may be regarded as the primary order parameter for this (isomorphic) phase transition. As can be seen, L exhibits the same behavior as R; the region of fit (135 K $< T <$ 175 K) is different, because of differing background effects in the two measurements, but the exponents and rounding regions are basically identical. The fact that R couples linearly to the order parameter justifies our use of resistivity data to perform the analysis in the critical regime.

Not shown in Fig. 1 is the first-order hysteresis. It shrinks from 14 K at $x = 0.200$ to 2 K at $x = 0.252$ and extrapolates to zero approximately at x_c, as do the magnitudes of the first-order jumps. Samples with $x \geq x_c$ exhibit a small hysteresis (1–2 K) which we believe is a polycrystalline strain effect. One obtains the same exponents and the same regions of fit for warming or cooling data; and theoretical reasons can be given to show that data taken along a path with a weakly varying pressure field will give rise to an unchanged exponent.[11]

The fact that mean-field behavior is observed so close to T_c has important implications, for it means that long-range forces dominate the critical behavior.[12] For the valence transition it is probably not electron screening interactions which give rise to the classical behavior, for the range of these is limited by the plasmon screening length. Anderson and Chui[4] have recently suggested that anharmonic effects associated with the large volume change (15%) at the valence transition are important in determing whether the transition is first or second order. Strain effects give rise to an effective interaction between ions which, being mediated by the lattice, is infinite ranged. This is similar in certain respects to the model proposed by Wagner and Horner[13] for hydrogen dissolved in niobium, where the hydrogen strains the host lattice in such a way as to lead to an infinite-range attractive interaction between hydrogen atoms, and a mean-field liquid-gas-type transition. We believe that a similar mechanism might be responsible for the observed classical critical behavior at the valence transition in $Ce_{1-x}Th_x$.

It is hoped that these results will lead to further theoretical effort towards understanding the driving mechanism for the valence transitions, and elucidating the spatial and temporal manifestations of the electroelastic coupling. On the experimental side it would be desirable to measure the acoustic properties of $Ce_{1-x}Th_x$ near the critical point and to attempt to measure critical exponents closer to T_c (i.e., $\epsilon < 10^{-3}$) in order to establish at least a lower bound on the range of the driving mechanism.

We wish to thank L. M. Falicov, B. I. Halperin, and T. M. Rice for helpful discussions.

*Work supported in part by the U. S. Army Research Office (Durham) and the U. S. Office of Naval Research.

[1]A. Jayaraman, P. Dernier, and L. D. Longinotti, Phys. Rev. B 11, 2783 (1975).

[2]T. Penney and F. Holtzberg, Phys. Rev. Lett. 34, 322 (1975).
[3]M. B. Maple, in *Magnetism and Magnetic Materials —1973,* AIP Conference Proceedings No. 18, edited by C. D. Graham and J. J. Rhyne (American Institute of Physics, New York, 1974), p. 447.
[4]P. W. Anderson and S. T. Chui, Phys. Rev. B 9, 3229 (1974).
[5]L. L. Hirst, J. Phys. Chem. Solids 35, 1285 (1974).
[6]R. A. Pollak, F. Holtzberg, J. L. Freeouf, and D. E. Eastman, Phys. Rev. Lett. 33, 820 (1974).
[7]For a review see R. Ramirez and L. M. Falicov, Phys. Rev. B 3, 2425 (1971).
[8]K. A. Gschneidner, Jr., R. O. Elliott, and R. R. McDonald, J. Phys. Chem. Solids 23, 555, 1191, 1201 (1962).
[9]M. Nicolas-Francillon, thesis, Faculté des Sciences d'Orsay, 1973 (unpublished).
[10]P. R. Roach, Phys. Rev. 170, 213 (1968).
[11]Details of sample preparation, data acquisition and analysis, and the results of other measurements will be presented in a forthcoming publication.
[12]V. L. Ginzburg. Fiz. Tverd. Tela 2, 2031 (1960) [Sov. Phys. Solid State 2, 1824 (1960)].
[13]H. Wagner and H. Horner, Advan. Phys. 23, 587 (1974).

Isotope Effect for Diffusion and the Structure of Liquid Water

Peter J. Dunlop
Department of Physical and Inorganic Chemistry, Adelaide University, Adelaide, South Australia 5001
(Received 17 March 1975)

Tracer diffusion data in the literature for HTO and DTO in both liquid H_2O and D_2O are interpreted in terms of a general equation usually employed to explain the isotope effect in solids. The results appear to be consistent with the stereo pictures of the time-dependent structure of liquid water which emerge from the molecular-dynamics study of Rahman and Stillinger.

In a recent paper Shankland, Dunlop, and Barr[1] applied the equations which are usually used to describe the "isotope effect" in solids to interpret the *very slight* isotope effect which they found for diffusion in several systems consisting of simple *unassociated* liquids. In all these systems it was found that essentially all the kinetic energy associated with the decomposition of the saddle-point configuration was lost to the surrounding molecules. The purpose of this short note is to indicate that quite a different result is obtained when the above equations are applied to liquid water which is believed to have a semi-ice structure.

Mills[2] has recently measured the temperature dependence of the tracer diffusion coefficients of HTO and DTO in H_2O and D_2O, respectively, and used the data of Longsworth[3] for the temperature dependence of the tracer diffusion coefficient of HDO in both H_2O and D_2O to derive the self-diffusion coefficients of both H_2O and D_2O. In addition, Mills[4] has discussed these coefficients in terms of a relation proposed by Le Claire[5] for the isotope effect in *gases*, and suggested that the definite isotope effect exhibited by his experimental data was approximately inversely proportional to the reduced mass of the system. This note indicates that a fundamental relation, which is often used to interpret the isotope effect in the *solid* state, may also be used to interpret the data of Mills[2] and Longsworth.[3]

The tracer diffusion coefficients chosen for analysis[2,3] are summarized in Table I, and cover a temperature range of 40°C.

The *general* equation used to describe the iso-

TABLE I. Tracer diffusion coefficients, $10^5 D_T$ (in $cm^2\ sec^{-1}$), for H_2O and D_2O. The first species at the top of each column is the isotopic tracer.

T (°C)	HTO/H_2O [a]	H_2O/H_2O [b]	DTO/D_2O [a]	D_2O/D_2O [b]
5	1.272	1.313	1.001	1.015
25	2.236	2.299	1.849	1.872
45	3.474	3.575	2.939	2.979

[a]Data of Mills, Ref. 2.
[b]Limiting tracer diffusion coefficients (self-diffusion coefficients) obtained by extrapolating the data of Mills (Ref. 2) and Longsworth (Ref. 3) to the normal molecular weights of H_2O and D_2O.